

Insulin Resistance Is Associated With Smaller Cortical Bone Size in Nondiabetic Men at the Age of Peak Bone Mass

Charlotte Verroken,¹ Hans-Georg Zmierzak,¹ Stefan Goemaere,¹ Jean-Marc Kaufman,¹ and Bruno Lapauw¹

¹Unit for Osteoporosis and Metabolic Bone Diseases, Department of Endocrinology, Ghent University Hospital, 9000 Ghent, Belgium

Context: In type 2 diabetes mellitus, fracture risk is increased despite preserved areal bone mineral density. Although this apparent paradox may in part be explained by insulin resistance affecting bone structure and/or material properties, few studies have investigated the association between insulin resistance and bone geometry.

Objective: We aimed to explore this association in a cohort of nondiabetic men at the age of peak bone mass.

Design, Setting, and Participants: Nine hundred ninety-six nondiabetic men aged 25 to 45 years were recruited in a cross-sectional, population-based sibling pair study at a university research center.

Main Outcome Measures: Insulin resistance was evaluated using the homeostasis model assessment of insulin resistance (HOMA-IR), with insulin and glucose measured from fasting serum samples. Bone geometry was assessed using peripheral quantitative computed tomography at the distal radius and the radial and tibial shafts.

Results: In age-, height-, and weight-adjusted analyses, HOMA-IR was inversely associated with trabecular area at the distal radius and with cortical area, periosteal and endosteal circumference, and polar strength strain index at the radial and tibial shafts ($\beta \leq -0.13$, $P < 0.001$). These associations remained essentially unchanged after additional adjustment for dual-energy X-ray absorptiometry–derived body composition, bone turnover markers, muscle size or function measurements, or adiponectin, leptin, insulin-like growth factor 1, or sex steroid levels.

Conclusion: In this cohort of nondiabetic men at the age of peak bone mass, insulin resistance is inversely associated with trabecular and cortical bone size. These associations persist after adjustment for body composition, muscle size or function, or sex steroid levels, suggesting an independent effect of insulin resistance on bone geometry. (*J Clin Endocrinol Metab* 102: 1807–1815, 2017)

The prevalence of type 2 diabetes mellitus (T2DM) has reached epidemic proportions. In addition to well-known microvascular and macrovascular complications, skeletal fragility is being increasingly recognized as

another important diabetes-associated condition. Indeed, despite having a comparable areal bone mineral density (aBMD) as measured by dual-energy X-ray absorptiometry (DXA), individuals with T2DM present with an

ISSN Print 0021-972X ISSN Online 1945-7197

Printed in USA

Copyright © 2017 Endocrine Society

Received 4 November 2016. Accepted 19 December 2016.

First Published Online 21 December 2016

Abbreviations: 25(OH)D, 25-hydroxyvitamin D; aBMD, areal bone mineral density; CSA, cross-sectional area; CTX, C-terminal telopeptide of type I collagen; CV, coefficient of variation; DXA, dual-energy X-ray absorptiometry; EC_{PC}, endosteal circumference additionally adjusted for periosteal circumference; FE₂, free estradiol; FT, free testosterone; HOMA-IR, homeostasis model assessment of insulin resistance; IGF-1, insulin-like growth factor 1; P1NP, procollagen type 1 N-terminal propeptide; pQCT, peripheral quantitative computed tomography; PTH, parathyroid hormone; SHBG, sex hormone-binding globulin; SSI_p, polar strength strain index; T2DM, type 2 diabetes mellitus; vBMD, volumetric bone mineral density; β , regression coefficient.

up to 1.7-fold increased risk of hip fractures as compared with nondiabetic subjects (1, 2).

This apparent paradox may in part be explained by indirect mechanisms, such as an increased risk of falls due to treatment-induced hypoglycemia and/or to diabetic retinopathy and neuropathy. Additionally, T2DM is often accompanied by obesity and excess body fat, which not only lead to higher impact forces during a fall, but also adversely affect bone characteristics (3, 4). Direct mechanisms may also play a role, as T2DM has been associated with alterations in bone structure and material properties, including cortical bone size deficits (5–7), higher cortical porosity (8–10), and compromised bone material strength (11). The pathophysiology underlying these structural and qualitative deficits remains incompletely understood. Diabetes-associated hyperglycemia, leading to the accumulation of advanced glycation end products, has been suggested to exert negative effects on bone metabolism and may be responsible for alterations of the bone material properties during the course of the disease. Nonetheless, the role of an adequate glycemic control in the prevention of diabetic bone fragility remains controversial (12). Alternatively, decreased bone strength may develop early as a consequence of the pathophysiology underlying T2DM, which is characterized by insulin resistance. Indeed, an inverse association of fasting insulin levels with periosteal circumference at the tibia has been reported in healthy adolescents (13), whereas insulin resistance [expressed as the homeostasis model assessment of insulin resistance (HOMA-IR)] correlated inversely with periosteal and endosteal circumference but positively with cortical thickness and trabecular microarchitecture at the ultradistal radius and tibia in nondiabetic postmenopausal women (14). Until now, our understanding of the mechanisms underlying these findings remains limited, and no studies have investigated this in adult men. The present study therefore aims to examine the associations of insulin resistance with bone geometry in a cohort of nondiabetic men at the age of peak bone mass. We hypothesized that (1) insulin resistance would be inversely associated with cortical bone size, and that (2) this association would be independent of body composition, muscle size or mechanical function, or sex steroid levels, suggesting a direct effect of insulin resistance on cortical bone accrual.

Subjects and Methods

Study design and population

This study is part of a population-based study designed to investigate determinants of peak bone mass in men, focusing on general lifestyle, sex hormone status, body composition, and genetic background (SIBLOS study). The detailed study design

has previously been described (15). Briefly, 1114 apparently healthy men aged 25 to 45 years, who had a brother within the same age range also willing to participate, were recruited from the population registries of the semirural to urban communities around Ghent, Belgium, between March 2002 and July 2010. All participants completed questionnaires about medical history, medication use, education, smoking, and calcium intake. Physical activity was scored using the questionnaire as proposed by Baecke *et al.* (16). Participants were screened for the presence of diabetes based on fasting glucose levels and medication use, but no participants were on antidiabetic drugs or had fasting glucose levels ≥ 7 mmol/L. After implementation of the exclusion criteria, including illnesses or medication use affecting body composition, sex hormone status, or bone metabolism, 1001 men were included in the study cohort. Five participants with nonfasting serum samples were additionally excluded from the present study, leaving a study sample of 996 men. The study protocol was approved by the Ethical Committee of the Ghent University Hospital, and written informed consent was obtained from all participants.

Biochemical measurements

Venous blood samples were obtained between 8:00 and 10:00 AM after an overnight fast. Serum samples were stored at -80°C until batch analysis. Commercial assays were used to determine serum levels of glucose (hexokinase method), insulin (Roche Diagnostics, Mannheim, Germany), leptin (Linco Research, St. Louis, MO), adiponectin (BioVendor, Brno, Czech Republic), insulin-like growth factor 1 (IGF-1; Diagnostic System Laboratories, Webster, TX and Cisbio Bioassays, Codolet, France), and sex hormone-binding globulin (SHBG; Orion Diagnostica, Espoo, Finland). C-terminal telopeptide of type I collagen (CTX), procollagen type 1 N-terminal propeptide (P1NP), N-mid fragment of osteocalcin, and intact parathyroid hormone (PTH) were measured using an electrochemiluminescence immunoassay (Roche Diagnostics, Mannheim, Germany). 25-Hydroxyvitamin D [25(OH)D] was determined after extraction by radioimmunoassay (DiaSorin, Stillwater, MN). Total testosterone and estradiol were determined using liquid chromatography–tandem mass spectrometry (AB Sciex 5500 triple-quadrupole mass spectrometer; AB Sciex, Toronto, ON, Canada). Free testosterone (FT) and free estradiol (FE2) were calculated from total testosterone, estradiol, SHBG, and albumin concentrations using a previously validated equation derived from the law of mass action (17, 18). Intraassay and interassay coefficients of variation (CVs) were $<10\%$ for all measurements. Insulin resistance was evaluated using HOMA-IR, calculated by multiplying insulin (mU/L) and glucose levels (mmol/L) and dividing the result by 22.5 (19). Higher HOMA-IR values indicate higher levels of insulin resistance.

Areal and volumetric bone mineral density and bone geometry

aBMD (mg/cm^2) was measured at the total body (without head), lumbar spine, and left proximal femur (total hip region and femoral neck) using DXA, with a Hologic QDR-4500A device (software version 11.2.1; Hologic, Bedford, MA). The CVs for spine and whole-body calibration phantoms were $<1\%$ as calculated from daily and weekly phantom measurements. Volumetric BMD (vBMD), bone geometry, and estimates of

bone strength were assessed using a peripheral quantitative computed tomography (pQCT) device (XCT-2000; Stratec Medizintechnik, Pforzheim, Germany). Cortical bone parameters, including cortical vBMD (mg/cm^3), cortical bone area (mm^2), periosteal circumference (mm), endosteal circumference (mm), and cortical thickness (mm) were measured at the dominant lower leg and forearm (tibial and radial shaft, 66% of bone length from distal end), with polar strength strain index (SSI_p, mm^3) calculated as previously described (20). Trabecular bone parameters, including trabecular vBMD (mg/cm^3) and trabecular bone area (mm^2) were measured at the nondominant forearm (distal radius, 4% of bone length from distal end). Single tomographic slices of 2.0-mm thickness were taken at a voxel size of 0.800 mm at the tibial and radial shaft and 0.590 mm at the distal radius, with a scan speed of 20 mm/second. Imaging and the calculation of numerical values were performed using the manufacturer's software package (version 5.4). Cross-sectional area (CSA) of the radius or tibia was determined after detecting the outer bone contour at a threshold of $280 \text{ mg}/\text{cm}^3$. At the distal radius, 55% of this cross-sectional bone area was peeled off to separate trabecular bone from the cortical shell. For determining cortical vBMD, the threshold was set at $710 \text{ mg}/\text{cm}^3$, whereas for trabecular bone it was set at $180 \text{ mg}/\text{cm}^3$. Periosteal and endosteal circumferences and cortical thickness were estimated using a circular ring model. The CV for the calibration phantom was $<1\%$ as calculated from daily measurements.

Body composition and muscle measurements

Body weight was measured to the nearest 0.1 kg in light indoor clothing without shoes. Standing height was measured to the nearest 0.1 cm using a wall-mounted Harpenden stadiometer (Holtain, Crymych, UK). Whole body soft tissue composition was measured using DXA; measurements include total body (minus head) fat and lean mass (kg). Muscle CSA (cm^2) was assessed at the dominant lower leg and forearm (66% of bone length from distal end) using pQCT, with a threshold below water equivalent linear attenuation set at $0.22/\text{cm}$. This threshold eliminated skin and fat mass with lower linear attenuation in the cross-sectional slice. From the remaining area, bone area was subtracted, showing the muscle at its maximum CSA. Isokinetic peak torque of the biceps and quadriceps muscle (Nm) was assessed at the dominant limb, using an isokinetic dynamometer (Biodex, New York, NY) at a preset constant angular velocity of $60^\circ/\text{second}$. Grip strength (kg) was measured at the dominant hand using an adjustable hand-held standard grip device (JAMAR hand dynamometer; Sammons & Preston, Bolingbrook, IL). The CV for grip strength was 4.08% as calculated from 3 repeated measurements for all participants, with the highest value used in further analyses. In a subset of participants, peak jump force (kN) was measured during multiple 1-legged hopping on the dominant limb, using a Leonardo Mechanograph ground reaction force platform (software version 4.2; Novotec Medical, Pforzheim, Germany).

Statistical analysis

Descriptives are expressed as mean \pm standard deviation or median (25th to 75th percentile) when criteria for normality were not fulfilled. Skewed variables (HOMA-IR, bone turnover markers, leptin, and adiponectin) were log transformed in subsequent linear models. Cross-sectional associations were

evaluated using linear mixed-effects modeling, with family number as a random effect and other predictor variables as fixed effects, taking the interdependence of measurements within families into account. A variance components residual correlation structure was used for random effects, and missing data were deleted listwise. Continuous variables were standardized to obtain standardized regression coefficients (β). Parameters of fixed effects were estimated using maximum likelihood estimation and reported as standardized β with their respective 95% confidence intervals. Unless stated otherwise, analyses were adjusted for age, height, and weight. To further explore whether the observed associations of HOMA-IR with bone geometry were independent of body composition, analyses were repeated with adjustment for total body lean and total body fat mass instead of weight. To explore whether the associations of HOMA-IR with bone geometry were independent of other metabolic parameters (leptin, adiponectin, IGF-1, or SHBG levels), muscle size or function, sex steroid levels, or bone turnover, these variables were alternately forced into the age-, height-, and weight-adjusted models. Analyses including endosteal circumference were additionally adjusted for periosteal circumference to provide an estimate of endosteal expansion independently of periosteal apposition (EC_{PC}). Associations were considered statistically significant at $P < 0.05$; all P values were 2-tailed. No adjustments were applied for multiple testing. All analyses were performed using SPSS version 23.0 (IBM, Armonk, NY).

Results

Characteristics of the study population

The study sample comprised 415 brother pairs, 89 singleton participants, 23 triplets, and 2 sets of 4 brothers. Their general characteristics, body composition and muscle parameters, and biochemical measurements are summarized in Table 1. Most participants (54.5%) had a normal body mass index, 37.3% were overweight, and 8.1% were obese. Mean relative body fat and lean mass were $19.6\% \pm 5.4\%$ and $76.9\% \pm 5.1\%$, respectively. Based on a HOMA-IR cut-off value of 2.17, which was recently proposed as the optimal cut-off value to predict incident T2DM in men (21), 198 participants (20.0%) would be defined as insulin resistant. Parameters reflecting bone geometry and strength are displayed in Table 2. The associations of body composition and muscle parameters with bone geometry in this population have previously been described (3, 15).

Associations of insulin resistance with bone geometry and strength

The associations of HOMA-IR with parameters reflecting bone geometry and strength are shown in Table 3. In age-, height-, and weight-adjusted analyses, HOMA-IR was inversely associated with trabecular area at the distal radius, with cortical area, periosteal and endosteal circumferences, and SSI_p at both the radial and tibial shafts, and with cortical thickness at the tibia. Additionally, positive associations with EC_{PC} were observed at both measurement sites. As compared with

Table 1. Characteristics of the Study Population (n = 996)

	Mean ± Standard Deviation or Median (25th–75th percentile)
General characteristics	
Age, y	34.5 ± 5.5
Height, cm	179.6 ± 6.5
Weight, kg	80.9 ± 11.6
Body mass index, kg/m ²	25.1 ± 3.5
Body composition and muscle parameters	
Total body fat mass, kg	15.4 (11.6–19.8)
Total body lean mass, kg	61.8 ± 6.7
Appendicular lean mass, kg	28.1 ± 3.4
Forearm muscle CSA, cm ²	45.1 ± 6.0
Lower leg muscle CSA, cm ²	82.6 ± 11.4
Grip strength, kg	52.7 ± 7.9
Biceps flexion torque, Nm	56.7 ± 10.1
Quadriceps extension torque, Nm	200.3 ± 42.1
Jump force, kN	2.3 ± 0.4
Biochemical parameters	
Fasting glucose, mmol/L	4.7 ± 0.5
Fasting insulin, pmol/L	44.0 (31.1–62.8)
HOMA-IR	1.35 (0.91–1.93)
Leptin, μg/L	4.1 (2.6–6.9)
Adiponectin, mg/L	8.3 (6.3–10.8)
IGF-1, ng/mL	346.7 ± 120.5
Osteocalcin, μg/L	21.8 (18.5–26.4)
P1NP, μg/L	50.8 (41.8–63.8)
CTX, μg/L	0.41 (0.31–0.52)
PTH, ng/L	33.4 (26.8–41.9)
25(OH)D, ng/mL	18.7 (14.2–23.9)

Data on jump force were available in 177 participants.

noninsulin-resistant men, insulin-resistant subjects presented with a smaller trabecular area at the distal radius, a smaller cortical thickness and increased endosteal expansion at the radial shaft, and a smaller cortical area, smaller periosteal and endosteal circumferences, and lower bone strength at both the radial and tibial shafts (Fig. 1).

HOMA-IR correlated inversely with 25(OH)D levels and the bone turnover markers osteocalcin, P1NP, and CTX in unadjusted analyses ($\beta = -0.17$, $P < 0.001$; $\beta = -0.13$, $P < 0.001$; $\beta = -0.13$, $P < 0.001$, and $\beta = -0.10$, $P = 0.001$), whereas a positive correlation was found with PTH ($\beta = 0.15$, $P < 0.001$). Except for the association with 25(OH)D, these associations however lost significance after adjustment for age, height, and weight. The previously described associations of HOMA-IR with bone geometry were unaffected when the bone markers were introduced into the statistical models (data not shown).

Possible confounders

After adjustment for lean and fat mass instead of weight, the inverse associations of HOMA-IR with

Table 2. Parameters Reflecting Bone Geometry and Strength (n = 996)

	Radius	Tibia
Trabecular area, mm ²	185.6 ± 25.6	—
Cortical area, mm ²	100.7 ± 13.5	364.9 ± 46.8
Cortical thickness, mm	2.47 ± 0.33	4.50 ± 0.55
Periosteal circumference, mm	48.8 ± 3.9	95.4 ± 6.1
Endosteal circumference, mm	33.2 ± 4.7	67.1 ± 6.9
SSI _p , mm ³	397.4 ± 81.8	3016.7 ± 523.2

Data are mean ± standard deviation.

trabecular area, cortical area, periosteal and endosteal circumferences, and SSI_p remained significant (Table 3). With the exception of a weak inverse interaction between HOMA-IR and fat mass for SSI_p at the radius ($P = 0.020$), we observed no interactions between HOMA-IR and fat or lean mass.

As shown in Table 4, the associations of HOMA-IR with trabecular and cortical bone geometry were unchanged when analyses were adjusted for physical activity, muscle torque, or grip strength. Adjustment for lean mass or muscle CSA attenuated the association of HOMA-IR with cortical thickness at the tibia, without affecting other associations. After adjustment for jump force, in the subgroup of 177 participants for whom these data were available, the inverse associations of HOMA-IR with periosteal and endosteal circumferences and SSI_p at the tibia remained significant, whereas associations with cortical area and EC_{PC} were attenuated. An inverse interaction between HOMA-IR and leg lean mass was observed for cortical area at the tibia (suggesting a weaker association between lean mass and cortical area in subjects with higher HOMA-IR values; $P = 0.022$), whereas a positive interaction was observed between HOMA-IR and jump force for periosteal circumference at the tibia ($P = 0.017$).

HOMA-IR correlated positively with IGF-1 and leptin ($\beta = 0.09$ and $\beta = 0.59$, both $P < 0.001$; unadjusted analyses) and inversely with adiponectin and SHBG ($\beta = -0.26$ and $\beta = -0.37$, both $P < 0.001$). Furthermore, HOMA-IR correlated inversely with FT ($\beta = -0.09$, $P = 0.003$) and positively with FE2 levels ($\beta = 0.08$, $P = 0.007$). The observed associations of HOMA-IR with bone geometry were unaltered after additional adjustment for adiponectin, IGF-1, SHBG, or FT and FE2 levels (data not shown). After adjustment for leptin, the associations of HOMA-IR with endosteal circumference at the radius, with cortical thickness at the tibia, and with EC_{PC} at both the radius and the tibia were attenuated, whereas other associations remained significant ($\beta = -0.08$, $P = 0.025$ for trabecular area; $\beta = -0.08$, $P = 0.023$ for endosteal circumference at the tibia; $\beta = -0.07$, $P \leq 0.037$ for

Table 3. Associations of HOMA-IR With Parameters Reflecting Bone Geometry and Strength

	Radius				Tibia			
	Model 1		Model 2		Model 1		Model 2	
	β (95% CI)	P	β (95% CI)	P	β (95% CI)	P	β (95% CI)	P
Trabecular area	-0.17 (-0.23;-0.10)	<0.001	-0.09 (-0.16;-0.03)	0.006	—	—	—	—
Cortical area	-0.19 (-0.26;-0.13)	<0.001	-0.09 (-0.15;-0.03)	0.006	-0.19 (-0.25;-0.13)	<0.001	-0.08 (-0.14;-0.02)	0.005
Cortical thickness	-0.07 (-0.14;0.003)	0.059	-0.02 (-0.09;0.05)	0.611	-0.09 (-0.16;-0.02)	0.010	-0.02 (-0.08;0.05)	0.645
Periosteal circumference	-0.20 (-0.27;-0.14)	<0.001	-0.11 (-0.18;-0.15)	0.001	-0.20 (-0.26;-0.15)	<0.001	-0.12 (-0.18;-0.07)	<0.001
Endosteal circumference	-0.14 (-0.21;-0.07)	<0.001	-0.09 (-0.16;-0.01)	0.018	-0.13 (-0.20;-0.07)	<0.001	-0.10 (-0.16;-0.03)	0.004
EC _{PC}	0.05 (0.02;0.08)	0.001	0.02 (-0.006;0.05)	0.119	0.06 (0.03;0.10)	0.001	0.03 (-0.008;0.06)	0.139
SSIp	-0.21 (-0.28;-0.15)	<0.001	-0.10 (-0.16;-0.04)	0.002	-0.21 (-0.27;-0.16)	<0.001	-0.11 (-0.16;-0.06)	<0.001

Model 1: model including HOMA-IR and age, height, and weight as predictors. Model 2: model including HOMA-IR and age, height, and total body lean and fat mass as predictors.

Abbreviation: CI, confidence interval.

cortical area at radius and tibia; $\beta \leq -0.08$, $P \leq 0.034$ for periosteal circumference at radius and tibia; $\beta \leq -0.08$, $P \leq 0.020$ for SSIp at radius and tibia). Inverse interactions between leptin and HOMA-IR (indicating stronger associations between HOMA-IR and bone geometry in subjects with higher leptin levels) were observed for trabecular area ($P = 0.024$), for cortical area

and endosteal circumference at the radius ($P = 0.001$ and $P = 0.022$), and for periosteal circumference and SSIp at the radius ($P = 0.001$ and $P < 0.001$) and tibia ($P = 0.041$ and $P = 0.028$).

HOMA-IR was not associated with smoking status [categorized as never ($n = 568$), former ($n = 214$), or current ($n = 214$) smoker; $P = 0.857$], and the observed

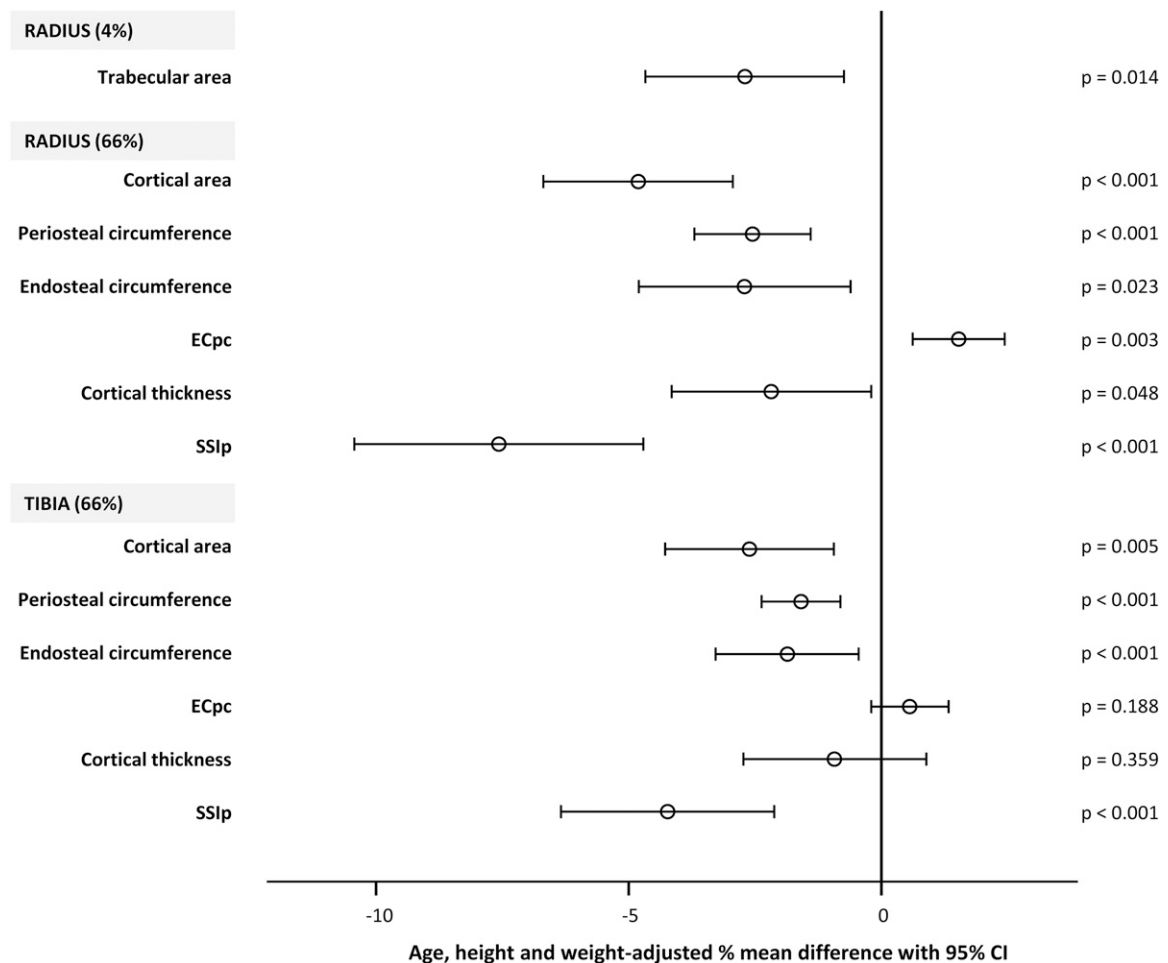


Figure 1. Age-, height-, and weight-adjusted relative differences in bone geometry and strength in insulin-resistant (HOMA-IR ≥ 2.17) vs noninsulin-resistant (HOMA-IR < 2.17) men.

Table 4. Associations of HOMA-IR With Parameters Reflecting Bone Geometry and Strength, Adjusted for Muscle Measurements or Physical Activity

	Arm Lean Mass-Adjusted β (95% CI)	Forearm Muscle CSA-Adjusted β (95% CI)	Grip Strength-Adjusted β (95% CI)	Biceps Torque-Adjusted β (95% CI)	Physical Activity-Adjusted β (95% CI)
Radius					
Trabecular area	-0.11 (-0.18; -0.05) ^a	-0.13 (-0.19; -0.06) ^b	-0.14 (-0.20; -0.08) ^b	-0.15 (-0.22; -0.08) ^b	-0.15 (-0.21; -0.08) ^b
Cortical area	-0.10 (-0.17; -0.04) ^a	-0.14 (-0.20; -0.08) ^b	-0.16 (-0.22; -0.10) ^b	-0.16 (-0.22; -0.09) ^b	-0.17 (-0.24; -0.10) ^b
Cortical thickness	-0.009 (-0.08; 0.07)	-0.05 (-0.12; 0.02)	-0.05 (-0.12; 0.02)	-0.05 (-0.12; 0.02)	-0.06 (-0.13; 0.01)
Periosteal circumference	-0.15 (-0.22; -0.08) ^b	-0.15 (-0.22; -0.09) ^b	-0.18 (-0.24; -0.11) ^b	-0.18 (-0.24; -0.11) ^b	-0.18 (-0.25; -0.11) ^b
Endosteal circumference	-0.12 (-0.20; -0.05) ^a	-0.11 (-0.18; -0.04) ^a	-0.12 (-0.19; -0.05) ^a	-0.12 (-0.20; -0.05) ^a	-0.12 (-0.20; -0.05) ^a
ECpc	0.03 (-0.006; 0.06)	0.04 (0.01; 0.07) ^a	0.05 (0.02; 0.08) ^a	0.05 (0.02; 0.08) ^a	0.05 (0.02; 0.08) ^a
SSI _p	-0.12 (-0.19; -0.06) ^b	-0.16 (-0.22; -0.10) ^b	-0.18 (-0.24; -0.12) ^b	-0.18 (-0.24; -0.12) ^b	-0.19 (-0.25; -0.12) ^b
	Leg Lean Mass-Adjusted β (95% CI)	Lower Leg Muscle CSA-Adjusted β (95% CI)	Jump Force-Adjusted β (95% CI)	Quadriceps Torque-Adjusted β (95% CI)	Physical Activity-Adjusted β (95% CI)
Tibia					
Cortical area	-0.10 (-0.16; -0.04) ^a	-0.15 (-0.20; -0.09) ^b	-0.09 (-0.25; 0.07)	-0.18 (-0.24; -0.12) ^b	-0.17 (-0.23; -0.11) ^b
Cortical thickness	-0.04 (-0.11; 0.03)	-0.06 (-0.12; 0.01)	0.05 (-0.12; 0.23)	-0.09 (-0.16; -0.02) ^c	-0.08 (-0.15; -0.01) ^c
Periosteal circumference	-0.12 (-0.18; -0.07) ^b	-0.18 (-0.23; -0.12) ^b	-0.26 (-0.43; -0.10) ^a	-0.19 (-0.25; -0.13) ^b	-0.19 (-0.25; -0.13) ^b
Endosteal circumference	-0.09 (-0.16; -0.02) ^c	-0.13 (-0.19; -0.06) ^b	-0.24 (-0.42; -0.06) ^a	-0.12 (-0.19; -0.06) ^b	-0.13 (-0.19; -0.06) ^b
ECpc	0.04 (0.002; 0.07) ^c	0.05 (0.01; 0.08) ^a	-0.008 (-0.10; 0.08)	0.06 (0.02; 0.09) ^a	0.06 (0.02; 0.09) ^a
SSI _p	-0.12 (-0.18; -0.07) ^b	-0.18 (-0.23; -0.12) ^b	-0.20 (-0.35; -0.05) ^c	-0.21 (-0.27; -0.15) ^b	-0.20 (-0.25; -0.14) ^b

Models are additionally adjusted for age, height, and weight. Data on jump force were available in 177 participants.

Abbreviation: CI, confidence interval.

^a $P < 0.01$.

^b $P < 0.001$.

^c $P < 0.05$.

associations of HOMA-IR with bone geometry were unchanged after adjustment for smoking status.

Associations of insulin resistance with areal and volumetric BMD

In age-, height-, and weight-adjusted analyses, HOMA-IR was inversely associated with aBMD at the total body ($\beta = -0.16$, $P < 0.001$), spine ($\beta = -0.10$, $P = 0.002$), total hip ($\beta = -0.12$, $P < 0.001$), and femoral neck ($\beta = -0.13$, $P < 0.001$); however, these associations lost significance after adjustment for body composition. Furthermore, no associations were observed between HOMA-IR and trabecular or cortical vBMD.

Discussion

In the present study, we investigated the associations of insulin resistance with bone geometry in nondiabetic men at the age of peak bone mass. Our results indicate that insulin resistance is inversely associated with trabecular and cortical bone size as well as with cortical bone strength, as reflected by inverse associations of HOMA-IR with trabecular area, cortical area, periosteal and endosteal circumferences, and SSI_p. These associations persist after adjustment for potential confounders,

including body composition, muscle size or function, and adiponectin, leptin, IGF-1, SHBG, or sex steroid levels, suggesting an independent adverse effect of insulin resistance on bone size and strength.

Our data corroborate the few other studies investigating the associations of insulin resistance with bone geometry. Inverse associations of HOMA-IR with periosteal and endosteal circumferences at the ultradistal radius and tibia have been reported in nondiabetic postmenopausal women (14), whereas fasting insulin levels were inversely associated with midtibial periosteal circumference and SSI in adolescents (13), and with midtibial total and cortical bone area and SSI in older adult men (22). Our findings are moreover largely in agreement with the existing literature on bone geometry in T2DM, with 2 pQCT studies reporting a smaller bone area at the distal and midshaft radius and tibia in individuals with vs without T2DM (5, 6). Studies using high-resolution pQCT at ultradistal sites have been more conflicting, with 1 study describing a smaller cortical area at the tibia (7) whereas others found no bone size differences (8, 10). However, these high-resolution pQCT studies are limited by very small sample sizes.

Several indirect mechanisms may underlie the inverse association between insulin resistance and bone size.

First, excess body fat is associated with a more unfavorable bone geometry (3, 23–26), at least when muscle parameters are taken into account. This might be explained by an altered adipokine secretion pattern and increased secretion of inflammatory cytokines, increased PTH and reduced 25(OH)D levels, a disturbed sex steroid profile, and/or a lower bone turnover, all of which are also associated with insulin resistance. However, in line with the findings of Sayers *et al.* (13), we demonstrated that the associations between HOMA-IR and bone geometry remained significant after adjustment for fat mass, although correlations were somewhat weaker in body composition– as compared with weight-adjusted models. Similar results were observed after adjustment for leptin, whereas adjustment for adiponectin, PTH or 25(OH)D levels, bone turnover markers, SHBG, or sex steroid levels did not affect the associations between insulin resistance and bone geometry. Thus, insulin resistance may exert its effects on bone at least in part independently of fat mass or adiposity-associated pathways. Moreover, we observed inverse interactions between HOMA-IR and leptin for several bone size measurements, indicating that the adverse effects of insulin resistance on bone geometry may even be aggravated in the presence of high leptin concentrations or *vice versa*.

Second, bone geometry is strongly dependent on mechanical load–induced strains, which primarily result from regional muscle contractions and for which muscle size and function measurements are common surrogates (15, 27–30). Even in nondiabetic subjects, muscle size and function are inversely associated with insulin resistance (31–33), so bone size deficits associated with insulin resistance could result from reduced strains. Furthermore, insulin resistance might modulate the muscle–bone relationship through downregulation of the anabolic effects of IGF-1 exposure in muscle tissue, as suggested in a cohort of prepubertal girls (34). In our study, adjustment for physical activity or muscle function, but not IGF-1, had a limited effect on the associations between insulin resistance and bone geometry. However, an inverse interaction between HOMA-IR and leg lean mass was observed for tibial cortical area, suggesting that the positive effects of muscle on bone geometry might be attenuated with increasing levels of insulin resistance. Thus, modulation of the muscle–bone relationship may play a role in explaining the relationship between insulin resistance and bone geometry at weight-bearing sites, underscoring the importance of physical activity in insulin-resistant subjects not only for general health, but also for bone health.

Other putative indirect mechanisms whereby insulin resistance may affect bone geometry involve a suggested

role of hyperinsulinemia in bone ageing (35, 36), and reduced blood flow to the bone tissue, which in turn adversely affects bone remodeling (37).

Impaired insulin signaling may also have direct effects on bone metabolism. Although the exact role of insulin in skeletal development remains incompletely understood, it has been shown that osteoblast-specific disruption of the insulin receptor leads to impaired osteoblast differentiation and reduced trabecular bone formation (38, 39). Moreover, experimental studies indicated that similar to skeletal muscle, hepatic, and adipose tissue, insulin resistance can develop in bone tissue, and that this compromised insulin signaling is associated with decreased bone remodeling (40). In our study, we indeed observed inverse correlations between insulin resistance and bone turnover markers, although they were not independent of body weight, and the associations between insulin resistance and bone geometry remained significant after adjustment for bone turnover. Future research is needed to elucidate whether insulin resistance exists in human bone and, if so, how it affects bone acquisition.

Our findings relate to a relatively young population, but if confirmed and prolonged over time, the adverse effects of insulin resistance on cortical bone geometry might impair future bone strength, which could in part explain the increased fracture risk observed in individuals with T2DM. Furthermore, our study supports the assumption that rather than being a late complication of T2DM and its associated chronic hyperglycemia, diabetic bone fragility may develop as an early consequence of its underlying pathophysiology. Given the cross-sectional design of this study, however, we acknowledge that rather than reflecting an ongoing phenomenon, the observed association between insulin resistance and bone geometry might also result from certain predisposing factors leading to both higher insulin resistance and a smaller bone size during growth.

A major strength of this study is the well-defined, population-based sample of adult men. Because all study subjects were between 25 and 45 years of age, we assume that they had already reached peak bone mass but were not yet subjected to major degenerative changes of the skeletal or the muscular system at the time of the study. The inclusion of apparently healthy subjects enabled us to investigate the effects of insulin resistance on bone geometry without the potentially confounding effects of chronic diseases. Participants furthermore underwent extensive phenotypic characterization with respect to bone geometry as well as possible confounders, using state-of-the-art techniques. An important limitation is that insulin sensitivity was not measured using the hyperinsulinemic-euglycemic clamp technique; however, HOMA-IR is considered a valid alternative to estimate

insulin sensitivity in epidemiologic studies and has been shown to predict incident T2DM (21, 41). No statistical correction was applied for multiple testing, but the reported associations were robust and internally coherent. Obviously, the cross-sectional design does not allow drawing conclusions about causality. As our study population only includes male subjects, the results of this study cannot be readily extrapolated to women, and future research is needed to assess whether insulin resistance also affects peak bone mass in women.

In conclusion, this study showed that in nondiabetic men at the age of peak bone mass, insulin resistance is inversely associated with trabecular as well as cortical bone size. These associations persist after adjustment for body composition, muscle size or function, and sex steroid levels, suggesting an independent effect of insulin resistance on bone geometry. Our findings support the hypothesis that adverse effects of insulin resistance on bone geometry contribute to the increased fracture incidence associated with T2DM, as well as the assumption that rather than being a late complication of T2DM, diabetic bone fragility may develop as an early consequence of its underlying pathophysiology.

Acknowledgments

The authors thank Kaatje Toye and Kathelyne Mertens for administrative and technical assistance, and all the volunteers for participation in the study.

Address all correspondence and requests for reprints to: Charlotte Verroken, MD, Unit for Osteoporosis and Metabolic Bone Diseases, Department of Endocrinology, Ghent University Hospital, De Pintelaan 185, 9K12IE, B-9000 Ghent, Belgium. E-mail: Charlotte.Verroken@UGent.be

The SIBLOS study was supported by a grant from the Fund for Scientific Research–Flanders (FWO–Vlaanderen, Grant G.0867.11).

Disclosure Summary: The authors have nothing to disclose.

References

- Vestergaard P. Discrepancies in bone mineral density and fracture risk in patients with type 1 and type 2 diabetes—a meta-analysis. *Osteoporos Int*. 2007;18(4):427–444.
- Janghorbani M, Van Dam RM, Willett WC, Hu FB. Systematic review of type 1 and type 2 diabetes mellitus and risk of fracture. *Am J Epidemiol*. 2007;166(5):495–505.
- Taes YE, Lapauw B, Vanbillemont G, Bogaert V, De Bacquer D, Zmierzak H, Goemaere S, Kaufman J-M. Fat mass is negatively associated with cortical bone size in young healthy male siblings. *J Clin Endocrinol Metab*. 2009;94(7):2325–2331.
- Mpalaris V, Anagnostis P, Goulis DG, Iakovou I. Complex association between body weight and fracture risk in postmenopausal women. *Obes Rev*. 2015;16(3):225–233.
- Melton III LJ, Riggs BL, Leibson CL, Achenbach SJ, Camp JJ, Boussein ML, Atkinson EJ, Robb RA, Khosla S. A bone structural basis for fracture risk in diabetes. *J Clin Endocrinol Metab*. 2008;93(12):4804–4809.
- Petit MA, Paudel ML, Taylor BC, Hughes JM, Strotmeyer ES, Schwartz AV, Cauley JA, Zmuda JM, Hoffman AR, Ensrud KE; Osteoporotic Fractures in Men (MrOs) Study Group. Bone mass and strength in older men with type 2 diabetes: the Osteoporotic Fractures in Men Study. *J Bone Miner Res*. 2010;25(2):285–291.
- Shu A, Yin MT, Stein E, Cremers S, Dworakowski E, Ives R, Rubin MR. Bone structure and turnover in type 2 diabetes mellitus. *Osteoporos Int*. 2012;23(2):635–641.
- Burghardt AJ, Issever AS, Schwartz AV, Davis KA, Masharani U, Majumdar S, Link TM. High-resolution peripheral quantitative computed tomographic imaging of cortical and trabecular bone microarchitecture in patients with type 2 diabetes mellitus. *J Clin Endocrinol Metab*. 2010;95(11):5045–5055.
- Patsch JM, Burghardt AJ, Yap SP, Baum T, Schwartz AV, Joseph GB, Link TM. Increased cortical porosity in type 2 diabetic postmenopausal women with fragility fractures. *J Bone Miner Res*. 2013;28(2):313–324.
- Yu EW, Putman MS, Derrico N, Abrishamian-Garcia G, Finkelstein JS, Boussein ML. Defects in cortical microarchitecture among African-American women with type 2 diabetes. *Osteoporos Int*. 2015;26(2):673–679.
- Farr JN, Drake MT, Amin S, Melton LJ III, McCready LK, Khosla S. In vivo assessment of bone quality in postmenopausal women with type 2 diabetes. *J Bone Miner Res*. 2014;29(4):787–795.
- Shanbhogue VV, Mitchell DM, Rosen CJ, Boussein ML. Type 2 diabetes and the skeleton: new insights into sweet bones. *Lancet Diabetes Endocrinol*. 2016;4(2):159–173.
- Sayers A, Lawlor DA, Sattar N, Tobias JH. The association between insulin levels and cortical bone: findings from a cross-sectional analysis of pQCT parameters in adolescents. *J Bone Miner Res*. 2012;27(3):610–618.
- Shanbhogue VV, Finkelstein JS, Boussein ML, Yu EW. Association between insulin resistance and bone structure in nondiabetic postmenopausal women. *J Clin Endocrinol Metab*. 2016;101(8):3114–3122.
- Lapauw BM, Taes Y, Bogaert V, Vanbillemont G, Goemaere S, Zmierzak HG, De Bacquer D, Kaufman JM. Serum estradiol is associated with volumetric BMD and modulates the impact of physical activity on bone size at the age of peak bone mass: a study in healthy male siblings. *J Bone Miner Res*. 2009;24(6):1075–1085.
- Baecke JA, Burema J, Frijters JE. A short questionnaire for the measurement of habitual physical activity in epidemiological studies. *Am J Clin Nutr*. 1982;36(5):936–942.
- Vermeulen A, Verdonck L, Kaufman JM. A critical evaluation of simple methods for the estimation of free testosterone in serum. *J Clin Endocrinol Metab*. 1999;84(10):3666–3672.
- Szulc P, Claustat B, Munoz F, Marchand F, Delmas PD. Assessment of the role of 17 β -oestradiol in bone metabolism in men: does the assay technique matter? The MINOS study. *Clin Endocrinol (Oxf)*. 2004;61(4):447–457.
- Matthews DR, Hosker JP, Rudenski AS, Naylor BA, Treacher DF, Turner RC. Homeostasis model assessment: insulin resistance and β -cell function from fasting plasma glucose and insulin concentrations in man. *Diabetologia*. 1985;28(7):412–419.
- Schoenau E, Neu CM, Rauch F, Manz F. The development of bone strength at the proximal radius during childhood and adolescence. *J Clin Endocrinol Metab*. 2001;86(2):613–618.
- Ghasemi A, Tohidi M, Derakhshan A, Hasheminia M, Azizi F, Hadaegh F. Cut-off points of homeostasis model assessment of insulin resistance, beta-cell function, and fasting serum insulin to identify future type 2 diabetes: Tehran Lipid and Glucose Study. *Acta Diabetol*. 2015;52(5):905–915.
- Laurent MR, Cook MJ, Gielen E, Ward KA, Antonio L, Adams JE, Decallonne B, Bartfai G, Casanueva FF, Forti G, Giwerzman A, Huhtaniemi IT, Kula K, Lean MEJ, Lee DM, Pendleton N, Punab M, Claessens F, Wu FCW, Vanderschueren D, Pye SR, O'Neill TW; EMAS Group. Lower bone turnover and relative bone deficits in men with metabolic syndrome: a matter of

- insulin sensitivity? The European Male Ageing Study. *Osteoporos Int*. 2016;27(11):3227–3237.
23. Gilsanz V, Chalfant J, Mo AO, Lee DC, Dorey FJ, Mittelman SD. Reciprocal relations of subcutaneous and visceral fat to bone structure and strength. *J Clin Endocrinol Metab*. 2009;94(9):3387–3393.
 24. Farr JN, Chen Z, Lisse JR, Lohman TG, Going SB. Relationship of total body fat mass to weight-bearing bone volumetric density, geometry, and strength in young girls. *Bone*. 2010;46(4):977–984.
 25. Wren TAL, Chung SA, Dorey FJ, Bluml S, Adams GB, Gilsanz V. Bone marrow fat is inversely related to cortical bone in young and old subjects. *J Clin Endocrinol Metab*. 2011;96(3):782–786.
 26. Bredella MA, Lin E, Gerweck AV, Landa MG, Thomas BJ, Torriani M, Bouxsein ML, Miller KK. Determinants of bone microarchitecture and mechanical properties in obese men. *J Clin Endocrinol Metab*. 2012;97(11):4115–4122.
 27. Frost HM. Bone “mass” and the “mechanostat”: a proposal. *Anat Rec*. 1987;219(1):1–9.
 28. Lebrasseur NK, Achenbach SJ, Melton LJ III, Amin S, Khosla S. Skeletal muscle mass is associated with bone geometry and microstructure and serum insulin-like growth factor binding protein-2 levels in adult women and men. *J Bone Miner Res*. 2012;27(10):2159–2169.
 29. Hardcastle SA, Gregson CL, Rittweger J, Crabtree N, Ward K, Tobias JH. Jump power and force have distinct associations with cortical bone parameters: findings from a population enriched by individuals with high bone mass. *J Clin Endocrinol Metab*. 2014;99(1):266–275.
 30. Verroken C, Zmierzak H-G, Goemaere S, Kaufman J-M, Lapauw B. Association of jumping mechanography-derived indices of muscle function with tibial cortical bone geometry. *Calcif Tissue Int*. 2016;98(5):446–455.
 31. Srikanthan P, Karlamangla AS. Relative muscle mass is inversely associated with insulin resistance and prediabetes. Findings from the third National Health and Nutrition Examination Survey. *J Clin Endocrinol Metab*. 2011;96(9):2898–2903.
 32. Lee S, Kim Y, White DA, Kuk JL, Arslanian S. Relationships between insulin sensitivity, skeletal muscle mass and muscle quality in obese adolescent boys. *Eur J Clin Nutr*. 2012;66(12):1366–1368.
 33. Gysel T, Calders P, Cambier D, Roman de Mettelinge T, Kaufman JM, Taes Y, Zmierzak H-G, Goemaere S. Association between insulin resistance, lean mass and muscle torque/force in proximal versus distal body parts in healthy young men. *J Musculoskelet Neuronal Interact*. 2014;14(1):41–49.
 34. Kindler JM, Pollock NK, Laing EM, Jenkins NT, Oshri A, Isaacs C, Hamrick M, Lewis RD. Insulin resistance negatively influences the muscle-dependent IGF-I-bone mass relationship in premenarcheal girls. *J Clin Endocrinol Metab*. 2016;101(1):199–205.
 35. Pinhas-Hamiel O, Benary D, Mazor-Aronovich K, Ben-Ami M, Levy-Shraga Y, Boyko V, Modan-Moses D, Lerner-Geva L. Advanced bone age and hyperinsulinemia in overweight and obese children. *Endocr Pract*. 2014;20(1):62–67.
 36. Lee HS, Shim YS, Jeong HR, Kwon EB, Hwang JS. The association between bone age advancement and insulin resistance in pre-pubertal obese children. *Exp Clin Endocrinol Diabetes*. 2015;123(10):604–607.
 37. Hinton PS. Role of reduced insulin-stimulated bone blood flow in the pathogenesis of metabolic insulin resistance and diabetic bone fragility. *Med Hypotheses*. 2016;93:81–86.
 38. Fulzele K, Riddle RC, DiGirolamo DJ, Cao X, Wan C, Chen D, Faugere M-C, Aja S, Hussain MA, Brüning JC, Clemens TL. Insulin receptor signaling in osteoblasts regulates postnatal bone acquisition and body composition. *Cell*. 2010;142(2):309–319.
 39. Ferron M, Wei J, Yoshizawa T, Del Fattore A, DePinho RA, Teti A, Ducy P, Karsenty G. Insulin signaling in osteoblasts integrates bone remodeling and energy metabolism. *Cell*. 2010;142(2):296–308.
 40. Wei J, Ferron M, Clarke CJ, Hannun YA, Jiang H, Blaner WS, Karsenty G. Bone-specific insulin resistance disrupts whole-body glucose homeostasis via decreased osteocalcin activation. *J Clin Invest*. 2014;124(4):1781–1793.
 41. Bonora E, Targher G, Alberiche M, Bonadonna RC, Saggiani F, Zenere MB, Monauni T, Muggeo M. Homeostasis model assessment closely mirrors the glucose clamp technique in the assessment of insulin sensitivity: studies in subjects with various degrees of glucose tolerance and insulin sensitivity. *Diabetes Care*. 2000;23(1):57–63.